doi:10.1016/j.jmb.2011.07.017 J. Mol. Biol. (2011) 413, 310–320

Contents lists available at www.sciencedirect.com

Journal of Molecular Biology

journal homepage: http://ees.elsevier.com.jmb

Quaternary Dynamics of αB-Crystallin as a Direct Consequence of Localised Tertiary Fluctuations in the C-Terminus

Andrew J. Baldwin[1]*, Gillian R. Hilton[2], Hadi Lioe[2], Claire Bagnéris[3], Justin L. P. Benesch[2]* and Lewis E. Kay[1]*

[1]*Departments of Molecular Genetics, Biochemistry and Chemistry, The University of Toronto, 1 Kings College Circle, Toronto, Ontario, Canada M5S 1A8*
[2]*Department of Chemistry, Physical and Theoretical Chemistry Laboratory, University of Oxford, South Parks Road, Oxford, Oxfordshire OX1 3QZ, UK*
[3]*Department of Crystallography and Institute of Structural and Molecular Biology, Birkbeck College London, Malet Street, London WC1E 7HX, UK*

Received 25 April 2011;
received in revised form
8 July 2011;
accepted 11 July 2011
Available online
3 August 2011

Edited by A. G. Palmer III

Keywords:
NMR spectroscopy;
small heat shock proteins (sHSPs);
chaperone;
mass spectrometry;
relaxation dispersion

The majority of proteins exist *in vivo* within macromolecular assemblies whose functions are dependent on dynamical processes spanning a wide range of time scales. One such assembly is formed by the molecular chaperone αB-crystallin that exists in a variety of exchanging oligomeric states, centred on a mass of approximately 560 kDa. For many macromolecular assemblies, including αB-crystallin, the inherent dynamics, heterogeneity and high mass contribute to difficulties in quantitative studies. Here, we demonstrate a strategy based on correlating solution-state nuclear magnetic resonance spectroscopy and mass spectrometry data to characterize simultaneously the organization and dynamics of the polydisperse αB-crystallin ensemble. We show that protomeric dimers assemble into oligomers via the binding of extended C-termini, with each monomer donating and receiving one terminus. Moreover, we establish that the C-termini undergo millisecond fluctuations that regulate the interconversion of oligomeric forms. The combined biophysical approach allows construction of an energy profile for a single monomer that completely describes the equilibrium dynamics of the ensemble. It also facilitates an analysis of dynamics spanning the millisecond to hour time scales and secondary to quaternary structural levels, and provides an approach for, obtaining simultaneously detailed structural, thermodynamic and kinetic information on a heterogeneous protein assembly.

*Corresponding authors. E-mail addresses:
ajb204@pound.med.utoronto.ca;
justin.benesch@chem.ox.ac.uk;
kay@pound.med.utoronto.ca.

Abbreviations used: MS, mass spectrometry; sHSP, small heat shock protein; TROSY, transverse relaxation optimized spectroscopy; CPMG, Carr–Purcell–Meiboom–Gill; HMQC, heteronuclear multiple-quantum correlation; PRE, paramagnetic relaxation enhancement; MTSL, [1-oxyl-2,2,5,5-tetramethyl-3-pyrroline-3-methyl]-methanethiosulfonate label; 2D, two dimensional.

Introduction

Proteins undergo structural fluctuations that span a wide range of scales in time and space that are often crucial for their cellular function.[1] The majority of cellular proteins assemble into multimeric complexes that dissociate, recombine, and interact with other cellular components.[2] An appreciation of the quaternary structures and dynamics of

0022-2836/$ - see front matter © 2011 Published by Elsevier Ltd.

these complexes is therefore essential for understanding their cellular biological function.[3]

Solution-state nuclear magnetic resonance spectroscopy (NMR) is particularly well suited to the study of the dynamics of proteins on a wide range of time scales.[4–6] Performing such experiments on large macromolecular complexes has, however, long proven a challenge due to their high mass and, hence, slow tumbling rates.[7] Nevertheless, by deuterating the protein, labelling only specified methyl groups with NMR active spin labels, and using optimised pulse sequences that preserve NMR signal, it is possible to study the structural and dynamical properties of even large macromolecular complexes with molecular masses in the hundreds of kilodaltons.[8]

Complementary to the residue-specific information available from NMR experiments, mass spectrometry (MS) data are capable of providing detailed information regarding the quaternary organization and dynamics of macromolecular assemblies.[9–11] Protein complexes can be transferred intact into the gas phase and, through capitalising on the high resolution of separation, the coexisting stoichiometries detected and their relative abundances assessed.[12] This, combined with a speed of analysis in real time starting on the seconds time scale, makes MS well suited for the study of the dynamics of heterogeneous protein complexes.[13–15] Here, we present a hybrid NMR and MS approach that combines the strengths of both techniques to study in detail the equilibrium fluctuations of a polydisperse molecular chaperone, αB-crystallin, so that site-specific motional information (from NMR) can be related to quaternary dynamics (from MS).

αB-crystallin is a mammalian member of the small heat shock proteins (sHSPs), a protein superfamily found in organisms spanning all biological kingdoms.[16] The sHSPs act to bind proteins destabilised during cellular stress and retain them in a folding competent form.[16–18] This prevents the aggregation and deposition of the unfolding proteins and instead ensures that they can be recovered by ATP-dependent chaperones.[16–18] This role of the sHSPs is central to the cellular protein homeostasis network,[19] and their malfunction is therefore implicated in a number of maladies that occur as a consequence of protein aggregation and accumulation.[20]

sHSPs are structurally composed of a dimeric β-sheet 'α-crystallin' core that spontaneously assembles into large oligomers via terminal interactions.[16–18] Specifically, X-ray structures of monodisperse sHSP oligomers, HSP16.9 from *Triticum aestivum*[21] and HSP16.5 from *Methanocaldococcus jannaschii*,[22] have revealed that a conserved IXI/V motif on the C-terminus of one monomer binds into a hydrophobic groove on the surface of an adjacent monomer such that two C-termini hold each monomer in place. Although X-ray crystallography derived structures are not available for αB-crystallin oligomers, the presence of similar interactions that stabilize the oligomeric structure is suggested by studies of truncated forms of the protein. Removal of the N- and C-terminal regions leads to the formation of predominantly dimeric species.[23–25] In cases where only the immediate C-terminal residues are removed, leading to a fragment extending from Met68 to Thr162, so that the IXI/V motif is still present, the crystal structure reveals dimers that polymerise by both donation and acceptance of the IPI residues.[26] Moreover, an NMR structure of αB-crystallin in the solid state indicates that these interactions are also present in the full-length protein.[27] Residues downstream of the IPI, a region known as the C-terminal extension (E164 to K175), are sufficiently flexible to be visible in fully protonated samples by means of solution-state NMR.[28,29]

αB-crystallin has proven a difficult target for structural biologists[30] due to a variable quaternary structure, populating oligomers containing between 10 and 40 subunits.[31,32] Furthermore, oligomers can interconvert freely, including with the αA-crystallin isoform and other sHSPs.[33] This capability for subunit exchange is putatively associated with chaperone activity.[16–18] In a companion paper, we have shown, from a quantitative analysis of the αB-crystallin population distributions obtained over a wide range of solution conditions, that this complex polydisperse ensemble can be explained in terms of just two types of interactions (intra- and interdimer) that are completely independent of oligomer stoichiometry.[34]

Here, we build on this work by examining αB-crystallin by means of solution-state NMR. We have measured ^{13}C–^{1}H methyl correlation TROSY (transverse relaxation optimized spectroscopy) spectra[35] showing one resonance for each of the nine Ile residues within the primary αB-crystallin sequence, confirming that there is one major conformational ensemble for all αB-crystallin monomers within the oligomers in solution.[34] In contrast to previous studies,[26,27] we demonstrate that, in solution, the C-terminal IPI is at most interacting only transiently with adjacent dimers. Moreover, using Carr–Purcell–Meiboom–Gill (CPMG) relaxation dispersion measurements,[36] we show that IPI undergoes a transition between ground and excited states on the millisecond time scale. The rates of exchange obtained from the NMR measurements can be correlated with those derived from MS measurements for the dissociation of monomers from the oligomers, using a suitable model in which a pair of C-terminal interactions are required for holding each monomer in position. This is in agreement with previous structural studies on αB-crystallin[26] and other sHSPs.[21,22,27] The subunit exchange process is thus limited by the simultaneous breaking of these interactions. Overall, our data support a model in

which the millisecond dynamics of the C-terminus underpin the quaternary dynamics of αB-crystallin that occur on the minute time scale and which, in turn, dictate the oligomeric distribution that is observed at equilibrium.

Results

Monomers within αB-crystallin oligomers occupy a single conformational ensemble in solution

Perdeuterated αB-crystallin containing $^{13}CH_3$ labels only at the isoleucine δ1 position was prepared, and ^{13}C–^{1}H heteronuclear multiple-quantum correlation (HMQC) spectra were recorded, exploiting a methyl-TROSY effect to enhance sensitivity.[37] Nine resonances are observed (Fig. 1a), as expected from the amino acid sequence of the monomer. In order to ensure that all of the nine cross-peaks in the spectrum are from Ile residues attached to the αB-crystallin oligomers and do not derive from smaller particles, such as monomers, we performed translational diffusion measurements.[41] The diffusion coefficients obtained by analysis of data from each of the nine peaks separately were the same and correspond to a particle with a hydrodynamic radius, R_H^{eff}, of ca 6 nm (Fig. 1b) This is similar to values published elsewhere[42] and is consistent with a species expected to diffuse as an approximate 30-mer ($R_H^{eff} \propto N^{0.23}$, where N is the number of residues).[38] This is in line with our MS measurements, which reveal a distribution of oligomers centred on a 28-mer.[34]

Together, this suggests that all monomers in solution possess the same basic structure regardless of the oligomer they transiently occupy. Moreover, peak positions change very little with temperature over a range from 20 to 50 °C (Fig. S1), demonstrating that temperature does not induce a substantial conformational rearrangement of the basic monomer structure.

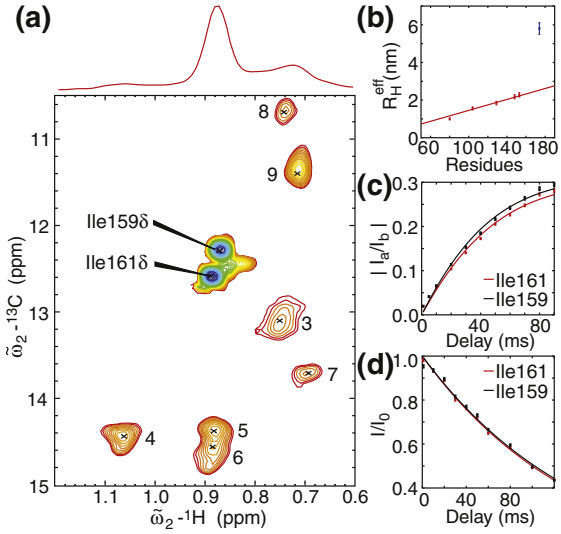

Fig. 1. I159/I161 of αB-crystallin are highly dynamic. (a) Methyl-TROSY spectrum of U-^{2}H,Ile-[$^{13}CH_3$-δ1]αB-crystallin, 18.8 T, 50 °C, pH 7. A 1D projection of the 2D data set is shown above the spectrum. The nine expected resonances are indicated (there are nine Ile per monomer), with the two especially sharp resonances assigned to positions 159 and 161 highlighted. (b) Hydrodynamic radii of a range of proteins measured using pulsed field gradient NMR. The hydrodynamic radius of a folded protein is expected to scale with the number of residues, N, according to $R_H^{eff} \propto N^{0.23}$ (continuous line).[38] The value measured for oligomeric αB-crystallin (blue) is 2.16 times larger than expected for a monomer of 175 residues, consistent with a complex composed of approximately 30 subunits. The globular, monomeric proteins used as calibrants were ABP1P-SH3 (80 residues), cytochrome C (104 residues), lysozyme (129 residues), calmodulin (148 residues) and myoglobin (153 residues). (c) Time dependencies of sums (I_b) and differences (I_a) of magnetization derived from methyl ^{1}H single-quantum transitions from which the product $S^2_{axis}\tau_C$ can be determined.[39] A value of 3.5 ns was obtained for both Ile159 and 161, consistent with their location in an unstructured region. (d) The decay of slowly relaxing proton magnetisation at 30 °C, pH 7, from which the transverse proton relaxation rate, R_2, can be determined.[40] The relaxation rates for Ile159 and 161 were found to be 6 s^{-1}.

The ^{13}C–^{1}H HMQC spectrum clearly shows that two of the nine Ile methyl-δ1 correlations are significantly more intense than the others (Fig. 1a); these can be assigned to I159/161 of the C-terminal IPI motif on the basis of mutagenesis experiments. Other experiments confirm that these Ile residues are highly dynamic. Firstly, ^{1}H spin relaxation experiments that probe the differential relaxation of methyl ^{1}H single-quantum transitions have been recorded (Fig. 1c). From these, the product $S^2_{axis}\tau_C$ is calculated,[39] where $0 \le S_{axis} \le 1$ is an order parameter that quantifies the amplitude of motions of the methyl axis, while τ_C is the assumed isotropic tumbling time for the particle. A value of $S^2_{axis}\tau_C = 3.5$ ns (30 °C) is obtained for both Ile methyl groups. Assuming $\tau_C \ge 150$ ns, as would be expected for a complex where the 'average' αB-crystallin particle size in solution is 30 monomers,[43] one obtains an upper bound for $S^2_{axis} = 0.02$. This is significantly lower than the average S^2_{axis} value, ≈0.5, that is measured for the Ile $C^{\delta 1}$–$C^{\gamma 1}$ axis in NMR spin relaxation studies on a series of folded proteins.[44] In addition, decay rates of the slowly relaxing methyl proton magnetization component[40] of the I159/I161 δ1-methyl groups have been measured, and the transverse relaxation rates obtained, $R_2 = 6$ s^{-1}, are also consistent with high mobility (Fig. 1d). Finally,

The C-terminal IPI is unbound in solution at ambient temperature

the carbon chemical shift of these peaks fall within 12.9 ± 1 ppm, the characteristic 'random-coil' region of isoleucine residues.[45]

The remaining seven correlations derive from residues originating from both the structured core of the protein and the N-terminus and are very broad under the solution conditions used in the present set of experiments. Their broadness likely stems from the oligomeric polydispersity and makes them unsuitable for the quantitative relaxation measurements described in this study, and they are therefore not considered in what follows.

To further probe the interactions formed by I159/I161 in αB-crystallin, we performed paramagnetic relaxation enhancement (PRE) NMR experiments. Paramagnetic labels lead to attenuation of NMR signals that derive from nearby nuclei,[46] and the resultant PRE values are quantified as the difference in proton transverse relaxation rates (R_2) in the presence and absence of paramagnetic label, in this case [1-oxyl-2,2,5,5-tetramethyl-3-pyrroline-3-methyl]-methanethiosulfonate label (MTSL), $\Gamma = R_2^{+\,\mathrm{MTSL}} - R_2^{-\,\mathrm{MTSL}}$ (Fig. 2a). PRE values vary as $\langle 1/r^6 \rangle$, where r is the distance between the unpaired electron of the paramagnet, and the NMR probe and the angular brackets denote averaging.[46] Therefore, at the very least, these measurements can provide qualitative measures of distance.

We have used the distance information obtained from PRE measurements to address whether the IXI interdimer interactions observed in X-ray structures of sHSPs *Mj*HSP16.5 and *Ta*HSP16.9[21,22] and in solid-state NMR studies of αB-crystallin[24] are also present in αB-crystallin oligomers in solution. MTSL was added to $^{13}CH_3$-labelled protein that had a mutation to cysteine at either position 135 or position 146 (only one position at a time; Fig. S2). Figure 2b illustrates the positions of the spin labels with respect to the I159/I161 probes in an X-ray structure of a truncated αB-crystallin construct[26] and reveals that both are within 10 Å of the hydrophobic groove that binds the C-terminus. PRE values between 10 and 41 s^{-1} were measured, depending on the position of the MTSL and the Ile residue (Table S1). If indeed these residues were fixed in solution, as suggested by the X-ray or solid-state NMR structure (Fig. 2a),[26,27] then the spin-label methyl–probe distances would range from 5 to 12 Å, giving rise to PRE values in excess of 2500 s^{-1} and resulting in the complete elimination of the I159/I161 peaks. The smaller than expected values are consistent, however, with the picture that emerges from the measured relaxation rates where these side chains are highly dynamic, sampling many conformations but still sufficiently restrained by an upstream 'tethering point' contact[29] that restrains these amino acids to a region around the hydrophobic groove on an adjacent dimer (Fig. 2b).

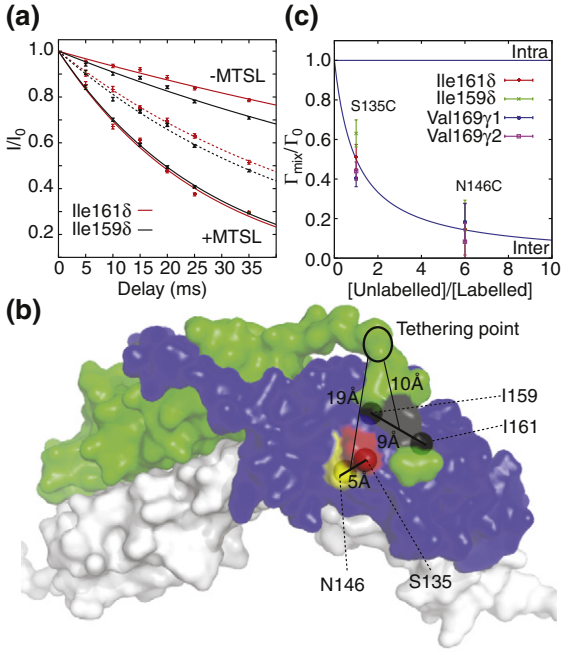

Fig. 2. Paramagnetic probes of I159, I161 interactions. (a) Decay curves of the slowly relaxing ^{1}H methyl signal intensity as a function of time[40] fitted to an equation of the form, $I = I_0 \exp(-R_2 t)$, where R_2 is the ^{1}H transverse relaxation rate, t is an experimental delay during which magnetization decays, I is the signal intensity at time t, and I_0 is the signal intensity at $t = 0$. Data were recorded at 30 °C, pH 7.0, either in the presence (+MTSL, rapid signal decay, continuous lines) or absence (−MTSL, slow signal decay, continuous lines) of MTSL spin label attached to position 135. In addition, experiments were performed on samples generated by mixing U-^{2}H,Ile-[$^{13}CH_3$-δ1], Leu, Val-[$^{13}CH_3$,$^{12}CD_3$]αB-crystallin + MTSL with αB-crystallin that is neither methyl, nor MTSL-labelled (dotted lines, with a mixture of MTS-labelled to MTS-unlabelled of 1:1). Data are shown for MTSL attached at position 135 as probed by Ile159 and 161. (b) An illustration of the relative positions of the two C-terminal isoleucines (shown in black) as well as the positions of MTS label, 135 (red) and 146 (yellow), in the structure of a truncated αB-crystallin construct, 68–162.[26] The black shading corresponds to the surface of the IPI motif (159–161). (c) Ratio of the PRE effect as a function of mixing with unlabelled protein. Measurements were made at two mixing ratios—1:1 (MTS at position 135) and 1:6 (MTS at position 146)—and data at both ratios were found to closely follow the trend expected for the case where the interaction between the methyl group of interest and the spin label is intermolecular.

The C-terminus of αB-crystallin forms interdimer contacts despite the fact that IPI is unbound

After PRE values were recorded, the NMR samples were subsequently mixed with αB-crystallin containing neither MTSL nor CH_3 labels and allowed

to equilibrate prior to the measurement of PREs in the mixed system (Fig. 2c and Table S1). In the simplest scenario, if intramolecular binding of the C-terminus occurs, then the magnitude of the PRE would not be expected to change significantly upon incubation. In contrast, if the interaction is intermolecular, then the magnitude of the PRE effect would be expected to decrease stoichiometrically according to $\frac{\Gamma_{mix}}{\Gamma_0} = \frac{1}{1+x}$, where the mixing ratio, [unlabelled protein]/[labelled protein]$=x$, Γ_{mix} and Γ_o are PRE rates measured on samples of αB-crystallin prepared as a mixture of MTS-labelled and MTS-unlabelled protein (Γ_{mix}) or as fully MTS-labelled (Γ_o). The data are in excellent agreement with the scaling expected for intermolecular interactions. Furthermore, within the dimer that forms the fundamental building block of the αB-crystallin oligomeric structure,[27] the IPI motif from one monomer cannot extend to the hydrophobic binding element of the second.[26] Together, this provides very strong evidence for interdimer contacts mediated by C-termini (Fig. 2c). While such interactions are also observed in all the high-resolution structures of sHSPs,[21,22,26,27] our PRE measurements have shown that these occur in αB-crystallin in solution.

Our NMR experiments indicate therefore that αB-crystallin dimers within an oligomer are 'cross-linked' via interactions involving C-terminal residues. However, the results presented here establish unequivocally that, unlike in the solid state, I159 and I161 are predominantly unbound in solution. This implies that the primary interactions between monomers on adjacent dimers involve residues that are upstream of positions 159/161.[26,29] Removal of a monomer from an oligomer must clearly involve breaking these C-terminal interactions.

The IPI region in the C-terminus undergoes dynamics on the millisecond time scale

In order to gain insight into the process by which these intra-oligomer C-terminal interactions are broken, we have recorded CPMG relaxation dispersion NMR experiments.[4] Unlike the other Ile residues in the structure, resonances from I159 and I161 decrease with increasing temperature, consistent with their involvement in a conformational exchange process on the millisecond time scale. This was confirmed by recording ^{13}C single-quantum CPMG dispersion profiles[47] for I159/I161 in the temperature range 30–50 °C at pH 5 and 9 (Fig. 3a). The profiles are well fit assuming a model of two-site chemical exchange involving a 'ground' NMR-observable state (G) and a second 'excited' conformation that is less stable and NMR unobservable (E), $G \underset{k_{EG}}{\overset{k_{GE}}{\rightleftharpoons}} E$ (Fig. 3a and Fig. S3). Data acquired at each pH were analysed globally to give values for the exchange rate, $k_{ex} = k_{GE} + k_{EG}$, the fractional population of the excited state, $p_E = 1 - p_G = \frac{k_{GE}}{k_{ex}} = \frac{[E]}{[E]+[G]}$, as well as residue-specific chemical shift differences between the two states (Fig. 3b and Table S2). The population of the excited state increases with temperature and is ca 1.5% at both 40 °C (pH 5) and 50 °C (pH 9). The $^{13}C^{\delta 1}$ chemical shifts of the excited state for both I159 and I161 are indicative of a more ordered structure than in the ground state.[45]

C-terminal millisecond dynamics are the basis of subunit exchange

Initially, one might assume that the NMR process reflects the dissociation of a monomer from an oligomer (k_e^-, see our companion paper)[34] so that the excited state, E, corresponds to a free monomer in

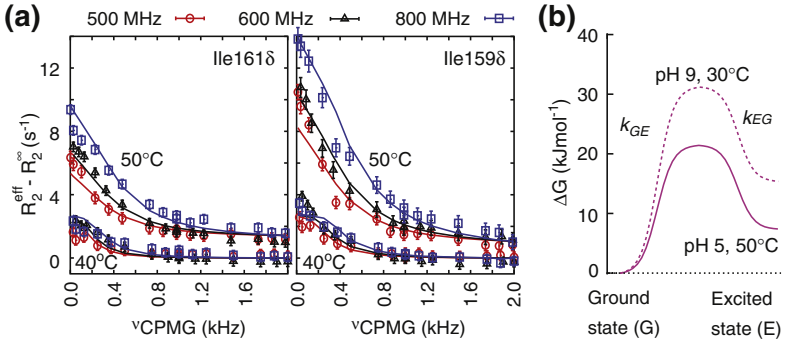

Fig. 3. The motions of I159 and I161 are critical for the control of quaternary dynamics. (a) $^{13}C^{\delta 1}$ CPMG relaxation dispersion profiles of I159/I161 measuring effective transverse relaxation rates (R_2^{eff}) as a function of the strength of an applied radiofrequency field (ν_{CPMG}). Data shown were recorded as a function of static magnetic field strength and temperature at pH 9. The value of the intrinsic relaxation rate (R_2^{∞}) has been subtracted from R_2^{eff} in the figure. (b) Dispersion data have been fitted to a model of two-site exchange to obtain the kinetics and thermodynamics of the exchange process involving I159/I161 from which free-energy surfaces can be constructed.

solution. If this were the case, then k_e^-, as measured by MS, would be equal to $k_{GE}=k_{ex}p_E$. NMR measurements at 40 °C (pH 9) indicate that k_{GE} is on the order of 10 s^{-1}, while dissociation rates measured by MS are less than ≈0.1 s^{-1}. The minor conformer is therefore clearly not the free monomeric state, and the exchange process observed by NMR cannot be attributed directly to monomer dissociation.

A second model is motivated by our finding that the C-termini of αB-crystallin link subunits together in solution (see above). In the high-resolution structures of sHSPs, similar interactions are found, with each of the monomers attached to an oligomer by a pair of such interdimer C-terminal 'flap' interactions: one interaction extending from a monomer to an adjacent binding site on a neighbouring dimer, a second involving the binding of a flap to the monomer in question.[21,22] Assuming that the process quantified by NMR is the removal of a single C-terminal flap, and that removal of adjacent C-termini are independent, then the rate for removal of two C-termini that would be required for dissociation of a monomer is calculated (see SI) to be

$$k_{2flap}^- = \frac{k_{flap}^- k_{flap}^-}{k_{flap}^- + k_{flap}^+} = k_{ex}p_E^2 \qquad (1)$$

where $k_{GE}=k_{flap}^-$ (the rate of removal of a single flap) and $k_{EG}=k_{flap}^+$ (the rate of flap association). Remarkably, the agreement between k_{2flap}^- and k_e^- (unpaired dissociation rate from MS, see companion paper)[34] is excellent over a temperature range of 30 °C and at both pH 5 and 9 (Fig. 4a).

Yet a third model is one that might be operative in the limit where the dimer interface is sufficiently strong such that exchange proceeds via dimer rather than monomer 'hopping'. Our model predicts that each dimer is held by four C-terminal interactions (two per monomer), with the rate for dimer dissociation given by

$$k_{4flap}^- = k_{2e}^- = \frac{\left(k_{flap}^-\right)^3}{\left(k_{flap}^- + k_{flap}^+\right)^2} = k_{ex}p_E^3 \qquad (2)$$

that follows directly from arguments given in the Supporting Information. The ratio $\frac{k_{4flap}^-}{k_{2flap}^-} = \frac{k_{2e}^-}{k_e^-} = p_E$ at its maximum is equal to 0.02 (pH 9, 50 °C) in the case of αB-crystallin. Thus, dimer hopping is 2

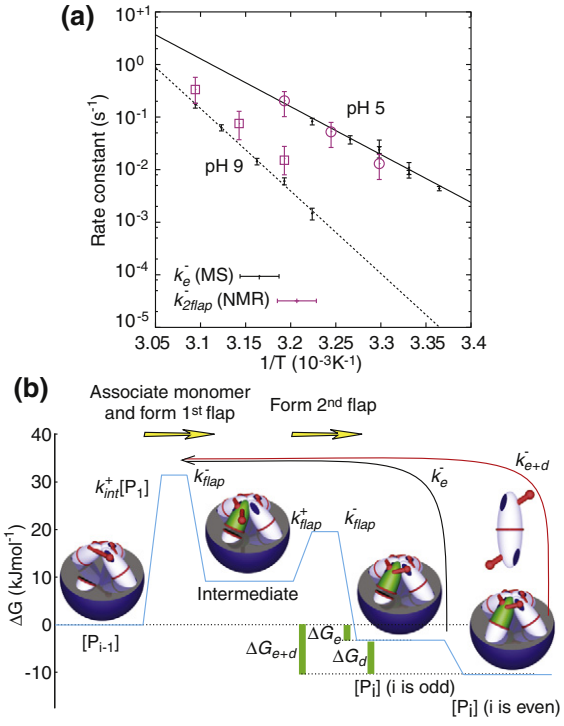

Fig. 4. Subunit exchange is controlled by the millisecond dynamics observed in the C-terminus. (a) NMR relaxation dispersion data from I159 and I161 obtained at three static magnetic field strengths (corresponding to ^{1}H resonance frequencies of 500, 600 and 800 MHz) were measured over a range of temperatures at both pH 5 and pH 9. These data were well described by a two-site model of chemical exchange, from which the ground-to-excited and excited-to-ground exchange rates k_{GE} and k_{EG}, respectively, were obtained. The subunit exchange rate of a single unpaired monomer as determined by MS (k_e^-) is in excellent agreement with the rate obtained from the NMR relaxation dispersion data using the model described in the text whereby k_{GE} (k_{EG}) corresponds to the rate of breaking(forming) an interdimer C-terminal flap interaction k_{flap}^- (k_{flap}^+). The rate for breaking a pair of flaps k_{2flap}^- can be calculated directly from k_{flap}^-, k_{flap}^+ (see the text and the Supporting Information). K_{2flap}^- (NMR) = k_e^- (MS) over a wide range of solution conditions, as expected for a model in which a pair of flap interactions must be broken prior to removal of a monomer from a given oligomer. (b) Energy profile of monomer dissociation from an αB-crystallin oligomer of arbitrary size, pH 9 at 50 °C. An oligomer is represented by the spherical particle, with interactions between a group of dimers within a given oligomer explicitly indicated. Each dimer in turn is represented by a white ellipsoid, with the dimer interface denoted by a red collar and internal monomers are denoted by half ellipsoids. Subunit exchange proceeds via the following pathway (left to right). A monomer (green) collides with an oligomer and forms a high-energy, sparsely populated intermediate state in which the monomer is held in place by only one of its two possible intermolecular C-terminal interactions (red). The second intermolecular C-terminal interaction is then formed rapidly. Such a mechanism supports rapid internal rearrangement allowing individual monomers within an oligomer to pair up, resulting in an optimally stable arrangement. The overall equilibrium size distribution and the quaternary dynamics of the system follow directly from such a scheme. Mathematical details are provided in the Supporting Information.

orders of magnitude slower than the corresponding rates for unpaired monomer exchange and is essentially inoperative in this system. It is worth emphasizing, moreover, that dimer exchange exclusively is not consistent with the size distribution profiles generated by MS, since particles with both odd and even numbers of monomers are observed.[34] Interestingly, in other sHSP systems that have been studied, dimer exchange is prevalent,[13] indicating that k^{-}_{e+d}, the dissociation rate of a monomer involving breaking of both dimer and edge interactions,[34] is much less than k^{-}_{2e} due to a strong dimer interface in these cases.

A single-monomer free-energy profile determines the quaternary structure and the dynamics of the system

By combining results from the MS and NMR measurements, it is possible to determine the shape of the free-energy surface controlling monomer association and dissociation (Fig. 4b and Supporting Information). In our model, dissociation proceeds from a bound, paired monomer through the rapid breaking of the dimeric interface, followed by breaking of the first C-terminal flap interaction to form an intermediate, and then finally removal of the second C-terminal flap. As the chemical shifts of the IPI residues in the excited state are consistent with a more ordered structure than in the ground state, it may be that the IPI residues form intramolecular contacts during the subunit dissociation process. The relative barrier heights and the stability of the intermediate strongly depend on both temperature and pH (Fig. S3); the profile in Fig. 4b pertains to pH 9, 50 °C.

Discussion

Analysis of profiles of the distribution of αB-crystallin stoichiometries as a function of pH and temperature reveals that their apparent complex, polydisperse nature can be well understood in terms of just two 'macroscopic' oligomer-independent interactions: the strength of the dimer interface and the strength of interdimer contacts.[34] Consistent with this finding, ^{13}C–^{1}H HMQC spectra of highly deuterated, methyl-protonated αB-crystallin protein samples establish that all monomers occupy essentially one conformational ensemble over a wide range of pH and temperature values. Similar observations have been made on plant sHSPs.[14,48]

In contrast to a recent study of intact αB-crystallin using solid-state NMR[27] and previous crystallographic studies of truncated constructs,[26] showing that the C-terminal Ile residues (I159/I161) are tightly bound to a hydrophobic groove on an adjacent dimer in solution, the NMR results reported here show that, in solution, the IXI/V motif is highly dynamic and not rigidly attached to the protein scaffold. ^{1}H transverse relaxation rates of I159/I161 δ1-methyl probes, measured order parameters and random-coil $^{13}C^{\delta 1}$ chemical shifts are consistent with the IPI moiety being entirely unstructured. Further, addition of a spin label to the hydrophobic groove does not eliminate the I159/I161 cross-peaks in HMQC spectra, although some attenuation is noted. These peaks would be completely suppressed if, however, the IPI unit were tightly bound to the groove, implying that, in solution, these residues interact transiently, at most, with the hydrophobic groove. The PREs measured for these residues decrease in a stoichiometric manner with addition of unlabelled protein, indicating that they derive from an intermolecular interaction. Together with measurements of the flexibility of the C-terminal extension,[28] these results establish that contrary to results in the solid state,[27,47] in the solution state the C-terminal region, including the IPI motif, is largely unstructured. While the IPI sequence is proximal to the hydrophobic groove on an adjacent dimer, these residues cannot be responsible for the contacts that contribute significantly to holding adjacent dimers together within an oligomer. It appears therefore that residues that are N-terminal to the IPI motif play this role.[29]

The Ile residues of the IPI sequence exchange between conformations on the millisecond time scale, an interconversion that can be studied directly by using CPMG relaxation dispersion measurements. Global fitting of the resulting dispersion profiles suggests a two-state process over a very wide range of pH and temperature values, and that the scaling of the rates with temperature at a given pH is well described by an Arrhenius relation. Remarkably, excellent agreement is obtained between the subunit exchange rates measured by means of MS, and those derived from NMR assuming that subunit exchange is caused by the breaking of a pair of C-terminal interactions. These interactions, rate limiting for subunit exchange in αB-crystallin, are observed in X-ray structures of monodisperse sHSPs[21,22] and in structures of the αB-crystallin protomers.[26] It is important to point out that the results of our kinetic analysis do not preclude additional contributions to the stability of the complex from other regions of the protein. The $^{13}C^{\delta 1}$ chemical shifts of the Ile probes in the transiently populated excited state are consistent with the IPI motif adopting a more ordered structure than the relatively disordered ground state, which may play a role in facilitating subunit exchange.

Correspondingly, the NMR results predict dimer exchange rates that are approximately 2 orders of magnitude slower than the dissociation kinetics quantified by means of MS. The NMR and MS results

are fully consistent with a model in which monomers, rather than dimers, or higher-order stoichiometries, are the exchanging units in the αB-crystallin system. This is in contrast to what is observed for other sHSP systems where dimer exchange is prevalent due to strong dimer interfaces.[13]

In a companion paper, we have discussed that chaperone activity can occur on a much faster time scale than that of subunit exchange reported by our MS experiments, implying that oligomer dissociation is not a prerequisite for the chaperone action of αB-crystallin.[34,49,50] This is consistent with results from studies on α-crystallin,[49] αA-crystallin[51] and HSP26 from *Saccharomyces cerevisiae*.[52] The latter protein has been shown to undergo a conformational rearrangement of its 'middle domain' at heat shock temperatures.[53] Such an activation mechanism is not the case for αB-crystallin because it lacks this domain, but also MS and NMR measurements indicate the presence of a single monomer conformation over the temperature range examined, 15–50 °C.

An alternative mechanism of regulating αB-crystallin chaperone activity has been postulated to involve the C-terminal IPI blocking substrate binding surfaces through its strong association with hydrophobic grooves on adjacent monomers, such that oligomerization is autoinhibitory of substrate binding.[21,27] Mutations in this region have been demonstrated to have aberrant behaviour *in vitro* and in cells,[54–56] giving rise to cataract formation and myopathy.[57–59] In this study, we have shown that the IXI/V motif of αB-crystallin is not tightly bound to hydrophobic grooves on neighbouring monomers, so chaperone function cannot be linked to the direct binding of these residues. They are, however, in relatively close proximity to the groove, suggesting that they may still act to shield this region from substrates. In this regard the fluctuations of the C-terminus that enable individual monomers to rearrange within the context of the oligomeric ensemble may well be important for substrate binding.

In summary, the present study demonstrates that a combined MS and NMR approach can be very beneficial for the analysis of complex macromolecular assemblies. MS provides a highly detailed view of 'macroscopic' quaternary structure and dynamics, whereas NMR gives complementary 'microscopic' secondary and tertiary structural information. Taken together, a comprehensive picture of αB-crystallin emerges in which quaternary dynamics on the minutes time scale are predicated by structural fluctuations on the millisecond time scale involving individual monomers. We envision that the type of methodology used herein will be applicable to the analysis of a wide range of large and complex macromolecular assemblies that have proven recalcitrant to more conventional biophysical characterization.

Methods

Protein production and purification

αB-crystallin was prepared by overexpression in *Escherichia coli* BL21(DE3) cells, with protein overexpression (IPTG induction) carried out overnight at 37 °C. Cells were harvested and lysed in 20 mM Tris (pH 8) buffer in the presence of a protease inhibitor cocktail (Roche) and passed down a Q column, eluting at 100 mM NaCl.[42] The fractions containing αB-crystallin were pooled, concentrated and passed down a 120-ml S200 gel-filtration column in 150 mM NaCl and 50 mM Tris (pH 8.0) where the protein eluted at 60 ml. U-^{2}H,Ile-[$^{13}CH_3$-δ1] protein was prepared by growing in D_2O and M9 media with [^{12}C,^{2}H]glucose as the sole carbon source and the precursor sodium α-ketobutyrate [$^{13}CH_3CD_2COCO_2Na$] (60 mg/L) added 1 h prior to induction.[60] U-^{2}H,Ile-[$^{13}CH_3$-δ1], Leu,Val-[$^{13}CH_3$,$^{12}CD_3$] αB-crystallin was generated as for Ile-labelled protein, with the addition of α-ketoisovalerate [$^{13}CH_3CD_3CDCOCO_2Na$] (80 mg/L) as described previously.[60]

NMR measurements

^{13}C–^{1}H correlation spectra were acquired using Varian NMR spectrometers operating at field strengths of 11.7, 14.0 and 18.8 T over a range of pHs (5–9) and temperatures (24–50 °C) using experiments optimised for large-molecular-weight proteins.[8,37,39,43,61] Translational diffusion coefficients were quantified for each resonance in the two-dimensional (2D) spectrum using a 2D ^{13}C–^{1}H correlation experiment that is based on a ^{15}N–$^{1}H^{N}$ pulse scheme[41] with a diffusion delay of 200 ms. To determine the mobility of individual methyl groups, we obtained proton R_2 relaxation rates as described previously.[40] In addition, values of the product $S^2_{axis}\tau_C$ were measured using the approach of Tugarinov *et al*. in which the time dependencies of sums (I_b) and differences (I_a) of magnetization derived from methyl ^{1}H single-quantum transitions are quantified.[39] The methyl resonances originating from I159, I161 and V169 were identified by producing a I159V/I161V U-^{2}H,Ile-[$^{13}CH_3$-δ1]-labelled sample and a I161A/V169S U-^{2}H,Ile-[$^{13}CH_3$-δ1], Leu,Val-[$^{13}CH_3$,$^{12}CD_3$]-labelled sample and observing which resonances were lost from the spectrum.

PRE measurements

U-^{2}H,Ile-[$^{13}CH_3$-δ1],Leu,Val-[$^{13}CH_3$,$^{12}CD_3$]-labelled cysteine mutants S135C and N146C of αB-crystallin were prepared by QuikChange site-directed

mutagenesis (Stratagene) and expressed and purified as above, with 5 mM DTT in all purification buffers. The buffer was exchanged to 100 mM KCl (pH 7) by successive rounds of centrifugation with centricon concentrators and incubated with 10-fold MTSL label (Toronto Research Chemicals) overnight before exchange into NMR buffer. Proton transverse relaxation rates, as described above, were determined in the presence ($R_2^{+\mathrm{MTSL}}$) and absence of MTSL ($R_2^{-\mathrm{MTSL}}$) so that the PRE could be quantified according to $\Gamma = R_2^{+\mathrm{MTSL}} - R_2^{-\mathrm{MTSL}}$.[46]

CPMG relaxation dispersion measurements

A set of constant-time single-quantum CPMG relaxation dispersion data sets were recorded[47] with $T_{\mathrm{relax}} = 40$ ms using a 1 mM αB-crystallin sample in 50 mM NaP_i D_2O at both pH 9 and pH 5 (corrected using pH = pH(measured) + 0.4) in the temperature range 30–50 °C. Seventeen CPMG frequencies between 25 and 2000 Hz were measured for each data set along with one reference where the constant-time CPMG element was removed. Data sets were obtained at three magnetic field strengths, 11.7, 14.0 and 18.8 T, with each spectrometer equipped with a room temperature (11.7, 18.8 T) or cryogenically cooled (14.0 T) probe. Eight scans per FID (free induction decay) were recorded, along with relaxation delays between scans of 2.5 s so that complete data sets (18 2D spectra) were generated in between 9 and 14 h (depending on the static magnetic field at which the data were recorded). Dispersion data were processed and analysed with the program NMRPipe[62] and signal intensities were quantified by using the program FuDA†. Relaxation dispersion data were interpreted by using a two-state exchange model and fitted using in-house software† following protocols described in detail previously.[63] Dispersion profiles at each pH were analysed for all residues together to extract global exchange parameters as well as residue specific chemical shift differences between ground and excited states and intrinsic relaxation rates.

Acknowledgements

We thank Carol V. Robinson, Christine Slingsby, Flemming Hansen, Guillaume Bouvignies, Julie Forman-Kay, Hong Lin, Christopher Waudby and Sarah Meehan for stimulating discussions. This work was supported by grants from the Canadian Institutes of Health Research and the Natural Sciences and Engineering Research Council of Canada (L.E.K.). A.J.B. acknowledges a postdoctoral fellowship, H.L. was a European Molecular Biology Organization fellow, J.L.P.B. is a Royal Society University Research Fellow and L.E.K. holds a Canada Research Chair in Biochemistry.

† http://pound.med.utoronto.ca/software

Supplementary Data

Supplementary data associated with this article can be found, in the online version, at doi:10.1016/j.jmb.2011.07.017

References

1. Karplus, M. & Kuriyan, J. (2005). Molecular dynamics and protein function. *Proc. Natl Acad. Sci. USA*, **102**, 6679–6685.
2. Robinson, C. V., Sali, A. & Baumeister, W. (2007). The molecular sociology of the cell. *Nature*, **450**, 973–982.
3. Alberts, B. (1998). The cell as a collection of protein machines: preparing the next generation of molecular biologists. *Cell*, **92**, 291–294.
4. Baldwin, A. J. & Kay, L. E. (2009). NMR spectroscopy brings invisible protein states into focus. *Nat. Chem. Biol.* **5**, 808–814.
5. Ishima, R. & Torchia, D. A. (2000). Protein dynamics from NMR. *Nat. Struct. Biol.* **7**, 740–743.
6. Mittermaier, A. K. & Kay, L. E. (2009). Observing biological dynamics at atomic resolution using NMR. *Trends Biochem. Sci.* **34**, 601–611.
7. Griswold, I. J. & Dahlquist, F. W. (2002). Bigger is better: megadalton protein NMR in solution. *Nat. Struct. Biol.* **9**, 567–568.
8. Sprangers, R., Velyvis, A. & Kay, L. E. (2007). Solution NMR of supramolecular complexes: providing new insights into function. *Nat. Methods*, **4**, 697–703.
9. Benesch, J. L. P., Ruotolo, B. T., Simmons, D. A. & Robinson, C. V. (2007). Protein complexes in the gas phase: technology for structural genomics and proteomics. *Chem. Rev*, **107**, 3544–3567.
10. Heck, A. J. (2008). Native mass spectrometry: a bridge between interactomics and structural biology. *Nat. Methods*, **5**, 927–933.
11. Sharon, M. & Robinson, C. V. (2007). The role of mass spectrometry in structure elucidation of dynamic protein complexes. *Annu. Rev. Biochem.* **76**, 167–193.
12. Benesch, J. L. P. & Ruotolo, B. T. (2011). Mass spectrometry: an approach come of age for structural and dynamical biology. *Curr. Opin. Struct. Biol.* in press. DOI:10.1016/j.sbi.2011.08.002.
13. Painter, A. J., Jaya, N., Basha, E., Vierling, E., Robinson, C. V. & Benesch, J. L. P. (2008). Real-time monitoring of protein complexes reveals their quaternary organization and dynamics. *Chem. Biol.* **15**, 246–253.
14. Stengel, F., Baldwin, A. J., Painter, A. J., Jaya, N., Basha, E., Kay, L. E. *et al.* (2010). Quaternary dynamics and plasticity underlie small heat shock protein chaperone function. *Proc. Natl Acad. Sci. USA*, **107**, 2007–2012.

15. Benesch, J. L., Aquilina, J. A., Baldwin, A. J., Rekas, A., Stengel, F., Lindner, R. A. *et al.* (2010). The quaternary organization and dynamics of the molecular chaperone HSP26 are thermally regulated. *Chem. Biol.* **17**, 1008–1017.
16. Haslbeck, M., Franzmann, T., Weinfurtner, D. & Buchner, J. (2005). Some like it hot: the structure and function of small heat-shock proteins. *Nat. Struct. Mol. Biol.* **12**, 842–846.
17. McHaourab, H. S., Godar, J. A. & Stewart, P. L. (2009). Structure and mechanism of protein stability sensors: chaperone activity of small heat shock proteins. *Biochemistry*, **48**, 3828–3837.
18. van Montfort, R., Slingsby, C. & Vierling, E. (2001). Structure and function of the small heat shock protein/α-crystallin family of molecular chaperones. *Adv. Protein Chem.* **59**, 105–156.
19. Balch, W. E., Morimoto, R. I., Dillin, A. & Kelly, J. W. (2008). Adapting proteostasis for disease intervention. *Science*, **319**, 916–919.
20. Ecroyd, H. & Carver, J. A. (2009). Crystallin proteins and amyloid fibrils. *Cell. Mol. Life Sci.* **66**, 62–81.
21. van Montfort, R. L., Basha, E., Friedrich, K. L., Slingsby, C. & Vierling, E. (2001). Crystal structure and assembly of a eukaryotic small heat shock protein. *Nat. Struct. Biol.* **8**, 1025–1030.
22. Kim, K. K., Kim, R. & Kim, S. H. (1998). Crystal structure of a small heat-shock protein. *Nature*, **394**, 595–599.
23. Bagnéris, C., Bateman, O. A., Naylor, C. E., Cronin, N., Boelens, W. C., Keep, N. H. & Slingsby, C. (2009). Crystal structures of α-crystallin domain dimers of αB-crystallin and Hsp20. *J. Mol. Biol.* **392**, 1242–1252.
24. Jehle, S., van Rossum, B., Stout, J. R., Noguchi, S. M., Falber, K., Rehbein, K. *et al.* (2009). αB-crystallin: a hybrid solid-state/solution-state NMR investigation reveals structural aspects of the heterogeneous oligomer. *J. Mol. Biol.* **385**, 1481–1497.
25. Clark, A. R., Naylor, C. E., Bagnéris, C., Keep, N. H. & Slingsby, C. (2011). Crystal structure of R120G disease mutant of human αB-crystallin domain dimer shows closure of a groove. *J. Mol. Biol.* **408**, 118–134.
26. Laganowsky, A., Benesch, J. L., Landau, M., Ding, L., Sawaya, M. R., Cascio, D. *et al.* (2010). Crystal structures of truncated αA and αB crystallins reveal structural mechanisms of polydispersity important for eye lens function. *Protein Sci.* **19**, 1031–1043.
27. Jehle, S., Rajagopal, P., Bardiaux, B., Markovic, S., Kuhne, R., Stout, J. R. *et al.* (2010). Solid-state NMR and SAXS studies provide a structural basis for the activation of αB-crystallin oligomers. *Nat. Struct. Mol. Biol.* **17**, 1037–1042.
28. Carver, J. A., Aquilina, J. A., Truscott, R. J. & Ralston, G. B. (1992). Identification by ^{1}H NMR spectroscopy of flexible C-terminal extensions in bovine lens α-crystallin. *FEBS Lett.* **311**, 143–149.
29. Treweek, T. M., Rekas, A., Walker, M. J. & Carver, J. A. (2010). A quantitative NMR spectroscopic examination of the flexibility of the C-terminal extensions of the molecular chaperones, αA- and αB-crystallin. *Exp. Eye Res.* **91**, 691–699.
30. Horwitz, J. (2009). α Crystallin: the quest for a homogeneous quaternary structure. *Exp. Eye Res.* **88**, 190–194.
31. Aquilina, J. A., Benesch, J. L., Bateman, O. A., Slingsby, C. & Robinson, C. V. (2003). Polydispersity of a mammalian chaperone: mass spectrometry reveals the population of oligomers in αB-crystallin. *Proc. Natl Acad. Sci. USA*, **100**, 10611–10616.
32. Aquilina, J. A., Benesch, J. L. P., Ding, L. L., Yaron, O., Horwitz, J. & Robinson, C. V. (2004). Phosphorylation of αB-crystallin alters chaperone function through loss of dimeric substructure. *J. Biol. Chem.* **279**, 28675–28680.
33. van den Oetelaar, P. J., van Someren, P. F., Thomson, J. A., Siezen, R. J. & Hoenders, H. J. (1990). A dynamic quaternary structure of bovine α-crystallin as indicated from intermolecular exchange of subunits. *Biochemistry*, **29**, 3488–3493.
34. Baldwin, A. J., Lioe, H., Robinson, C. V., Kay, L. E. & Benesch, J. L. P. αB-crystallin polydispersity is a consequence of unbiased quaternary dynamics. *J. Mol. Biol.* in press. DOI:10.1016/j.jmb.2011.07.016.
35. Tugarinov, V., Hwang, P. M., Ollerenshaw, J. E. & Kay, L. E. (2003). Cross-correlated relaxation enhanced ^{1}H^{13}C NMR spectroscopy of methyl groups in very high molecular weight proteins and protein complexes. *J. Am. Chem. Soc.* **125**, 10420–10428.
36. Palmer, A. G., Grey, M. J. & Wang, C. (2005). Solution NMR spin relaxation methods for characterizing chemical exchange in high-molecular-weight systems. *Methods Enzymol.* **394**, 430–465.
37. Ollerenshaw, J. E., Tugarinov, V. & Kay, L. E. (2003). Methyl TROSY: explanation and experimental verification. *Magn. Reson. Chem.* **41**, 843–852.
38. Wilkins, D. K., Grimshaw, S. B., Receveur, V., Dobson, C. M., Jones, J. A. & Smith, L. J. (1999). Hydrodynamic radii of native and denatured proteins measured by Pulse field gradient {NMR} techniques. *Biochemistry*, **38**, 16424–16431.
39. Tugarinov, V., Sprangers, R. & Kay, L. E. (2007). Probing side-chain dynamics in the proteasome by relaxation violated coherence transfer NMR spectroscopy. *J. Am. Chem. Soc.* **129**, 1743–1750.
40. Tugarinov, V. & Kay, L. E. (2006). Relaxation rates of degenerate ^{1}H transitions in methyl groups of proteins as reporters of side-chain dynamics. *J. Am. Chem. Soc.* **128**, 7299–7308.
41. Choy, W. Y., Mulder, F. A., Crowhurst, K. A., Muhandiram, D. R., Millett, I. S., Doniach, S. *et al.* (2002). Distribution of molecular size within an unfolded state ensemble using small-angle X-ray scattering and pulse field gradient NMR techniques. *J. Mol. Biol.* **316**, 101–112.
42. Meehan, S., Knowles, T. P., Baldwin, A. J., Smith, J. F., Squires, A. M., Clements, P. *et al.* (2007). Characterisation of amyloid fibril formation by small heat-shock chaperone proteins human αA-, αB- and R120G αB-crystallins. *J. Mol. Biol.* **372**, 470–484.
43. Sprangers, R. & Kay, L. E. (2007). Quantitative dynamics and binding studies of the 20S proteasome by NMR. *Nature*, **445**, 618–622.
44. Mittermaier, A., Kay, L. E. & Forman-Kay, J. D. (1999). Analysis of deuterium relaxation-derived methyl axis

order parameters and correlation with local structure. *J. Biomol. NMR*, **13**, 181–185.
45. Hansen, D. F., Neudecker, P. & Kay, L. E. (2010). Determination of isoleucine side-chain conformations in ground and excited states of proteins from chemical shifts. *J. Am. Chem. Soc.* **132**, 7589–7591.
46. Clore, G. M., Tang, C. & Iwahara, J. (2007). Elucidating transient macromolecular interactions using paramagnetic relaxation enhancement. *Curr. Opin. Struct. Biol.* **17**, 603–616.
47. Lundstrom, P., Vallurupalli, P., Religa, T. L., Dahlquist, F. W. & Kay, L. E. (2007). A single-quantum methyl ^{13}C-relaxation dispersion experiment with improved sensitivity. *J. Biomol. NMR*, **38**, 79–88.
48. Wintrode, P. L., Friedrich, K. L., Vierling, E., Smith, J. B. & Smith, D. L. (2003). Solution structure and dynamics of a heat shock protein assembly probed by hydrogen exchange and mass spectrometry. *Biochemistry*, **42**, 10667–10673.
49. Augusteyn, R. C. (2004). Dissociation is not required for α-crystallin's chaperone function. *Exp. Eye Res.* **79**, 781–784.
50. Bova, M. P., Ding, L. L., Horwitz, J. & Fung, B. K. (1997). Subunit exchange of αA-crystallin. *J. Biol. Chem.* **272**, 29511–29517.
51. Aquilina, J. A., Benesch, J. L., Ding, L. L., Yaron, O., Horwitz, J. & Robinson, C. V. (2005). Subunit exchange of polydisperse proteins: mass spectrometry reveals consequences of αA-crystallin truncation. *J. Biol. Chem.* **280**, 14485–14491.
52. Franzmann, T. M., Wuhr, M., Richter, K., Walter, S. & Buchner, J. (2005). The activation mechanism of Hsp26 does not require dissociation of the oligomer. *J. Mol. Biol.* **350**, 1083–1093.
53. Franzmann, T. M., Menhorn, P., Walter, S. & Buchner, J. (2008). Activation of the chaperone Hsp26 is controlled by the rearrangement of its thermosensor domain. *Mol. Cell*, **29**, 207–216.
54. Hayes, V. H., Devlin, G. & Quinlan, R. A. (2008). Truncation of αB-crystallin by the myopathy-causing Q151X mutation significantly destabilizes the protein leading to aggregate formation in transfected cells. *J. Biol. Chem.* **283**, 10500–10512.
55. Treweek, T. M., Ecroyd, H., Williams, D. M., Meehan, S., Carver, J. A. & Walker, M. J. (2007). Site-directed mutations in the C-terminal extension of human αB-crystallin affect chaperone function and block amyloid fibril formation. *PLoS One*, **2**, e1046.
56. Zhang, H., Rajasekaran, N. S., Orosz, A., Xiao, X., Rechsteiner, M. & Benjamin, I. J. (2010). Selective degradation of aggregate-prone CryAB mutants by HSPB1 is mediated by ubiquitin–proteasome pathways. *J. Mol. Cell. Cardiol.* **49**, 918–930.
57. Berry, V., Francis, P., Reddy, M. A., Collyer, D., Vithana, E., MacKay, I. *et al.* (2001). αB crystallin gene (CRYAB) mutation causes dominant congenital posterior polar cataract in humans. *Am. J. Hum. Genet.* **69**, 1141–1145.
58. Selcen, D. & Engel, A. G. (2003). Myofibrillar myopathy caused by novel dominant negative αB-crystallin mutations. *Ann. Neurol.* **54**, 804–810.
59. Inagaki, N., Hayashi, T., Arimura, T., Koga, Y., Takahashi, M., Shibata, H. *et al.* (2006). αB-crystallin mutation in dilated cardiomyopathy. *Biochem. Biophys. Res. Commun.* **342**, 379–386.
60. Ruschak, A. M. & Kay, L. E. (2010). Methyl groups as probes of supra-molecular structure, dynamics and function. *J. Biomol. NMR*, **46**, 75–87.
61. Tugarinov, V., Hwang, P. M., Ollerenshaw, J. E. & Kay, L. E. (2003). Cross-correlated relaxation enhanced ^{1}H–^{13}C NMR spectroscopy of methyl groups in very high molecular weight proteins and protein complexes. *J. Am. Chem. Soc.* **125**, 10420–10428.
62. Delaglio, F., Grzesiek, S., Vuister, G. W., Zhu, G., Pfeifer, J. & Bax, A. (1995). NMRPipe: a multidimensional spectral processing system based on UNIX pipes. *J. Biol. NMR*, **V6**, 277–293.
63. Vallurupalli, P., Hansen, D. F., Stollar, E., Meirovitch, E. & Kay, L. E. (2007). Measurement of bond vector orientations in invisible excited states of proteins. *Proc. Natl Acad. Sci. USA*, **104**, 18473–18477.